Zonal-mean zonal wind and Hadley circulation

Kevin M Grise^a and William JM Seviour^b, ^aUniversity of Virginia, Charlottesville, VA, United States; ^bUniversity of Exeter, Exeter, United Kingdom

© 2025 Elsevier Inc. All rights are reserved, including those for text and data mining, Al training, and similar technologies.

Introduction	1
Climatology	1
Internal variability	3
Historical trends	5
Conclusion	8
References	8

Abstract

This chapter reviews the representation of atmospheric winds averaged over all longitudes (zonal-mean atmospheric circulation) in the latest generation of global climate models, focusing on the rendition of natural climate variability and recent trends in the models' historical (20th –21st century) simulations. In general, models well capture the climatology, variability, and recent observed trends in the zonal-mean atmospheric circulation, including the meridional overturning Hadley circulation in the tropics and the west-to-east subtropical and midlatitude (eddy-driven) jet streams. However, notable biases remain for some circulation features, particularly those linked to multi-decadal variability in the ocean.

Key points

- Global climate models well capture the climatology, variability, and recent observed trends in the zonal-mean atmospheric circulation.
- Models' representation of circulation variability is affected by how well they capture modes of natural climate variability.
- It is challenging to compare models' forced circulation trends over recent decades with observed trends, which are affected by both natural variability and climate change.

Introduction

This chapter reviews the representation of atmospheric winds averaged over all longitudes (i.e., the zonal-mean atmospheric circulation) in the latest generation of computer models that are used to make projections for Earth's climate system (those from phase 6 of the Coupled Model Intercomparison Project, or CMIP6). The chapter first reviews the long-term average (climatological) circulation and then assesses its representation in models. It then addresses the ability of models to capture internal variability in the circulation on weekly to multi-decadal timescales. The chapter concludes with an assessment of the models' ability to capture recent observed circulation trends in the late 20th and early 21st centuries.

Climatology

Earth's zonal-mean atmospheric circulation is often described using the three-cell model. The black contours in Fig. 1a show the observed annual-mean meridional overturning circulation, as represented by the ERA5 reanalysis. Positive values (solid contours) indicate clockwise overturning cells, and negative values (dashed contours) indicate counterclockwise overturning cells. In each hemisphere, there are three cells: a Hadley cell with rising motion in the deep tropics and sinking motion in the subtropics, a Ferrel cell with rising motion near 60° latitude and sinking motion at the pole (not pictured in Fig. 1).

Of the three cells, the Hadley cells possess the strongest meridional overturning circulation. The rising branch of the Hadley circulation is associated with the Intertropical Convergence Zone (ITCZ), a region of intense deep convective activity near the Equator. In the annual mean, the rising branch of the Hadley circulation (and ITCZ) is located around 5°N, as there is net energy transport by the oceanic circulation from the Southern to Northern Hemisphere (Schneider et al., 2014). The annual-mean cross-equatorial Hadley circulation with rising motion around 5°N and sinking motion in the Southern Hemisphere (SH) subtropics allows the atmosphere to flux energy southward across the Equator, to help to compensate for the northward energy transport by the ocean. However, the annual-mean structure of the Hadley circulation is only observed in equinox seasons (Dima and Wallace, 2003). Across the seasonal cycle, the Hadley circulation is dominated by cross-equatorial winter cells, with rising

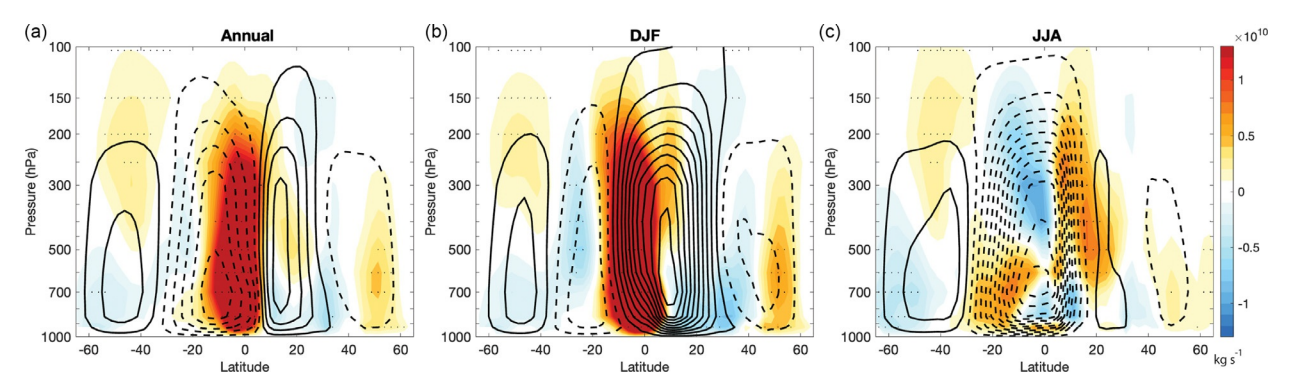


Fig. 1 1980–2010 climatology of mean meridional mass stream function for (a) annual-mean, (b) December–February (DJF) mean, and (c) June–August (JJA) mean. Thick black contours denote ERA5 climatology (contour interval: 2.0 × 10¹⁰ kg s⁻¹, dashed contours negative). Color shading indicates CMIP6 multi-model-mean bias based on the historical runs of 25 CMIP6 models. Stippling indicates where over 80% of the models agree on the sign of the bias.

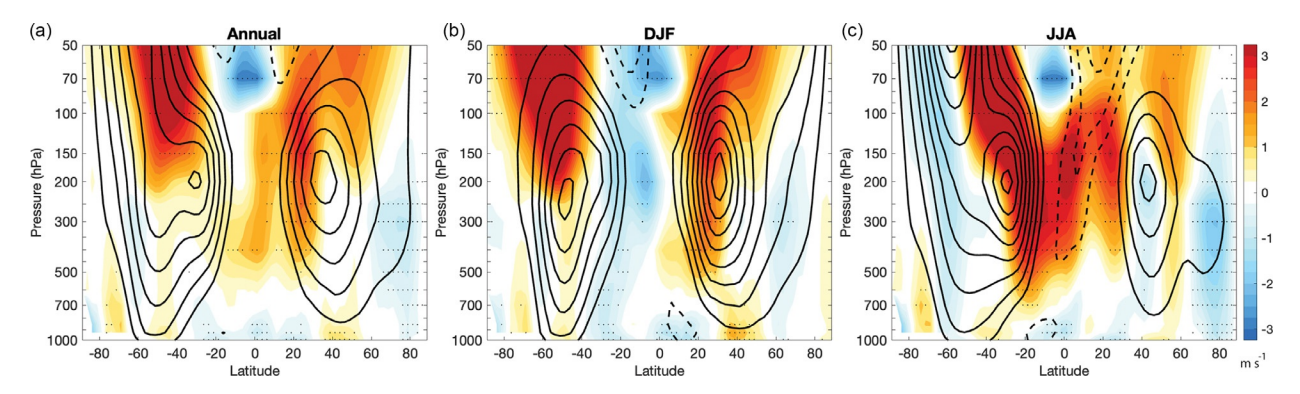


Fig. 2 1980–2010 climatology of zonal-mean zonal wind for (a) annual-mean, (b) December–February (DJF) mean, and (c) June–August (JJA) mean. Thick black contours denote ERA5 climatology (contour interval: 5 m s⁻¹, dashed contours negative). Color shading indicates CMIP6 multi-model-mean bias based on the historical runs of 25 CMIP6 models. Stippling indicates where over 80% of the models agree on the sign of the bias.

motion in the summer hemisphere's tropics and sinking motion near 30° latitude in the winter hemisphere (Figs. 1b-c). The summer hemisphere Hadley cells are decidedly weaker, particularly in the Northern Hemisphere (NH).

As could be expected from the conservation of angular momentum, the poleward moving air in the upper tropospheric branches of the Hadley circulation drives strong west-to-east subtropical jet streams in the subtropical upper troposphere near 30° latitude, with the subtropical jets being stronger in the winter hemisphere due to the dominant cross-equatorial cell (Fig. 2). Similarly, equatorward moving air in the lower troposphere drives east-to-west trade winds near the surface. However, angular momentum is not actually conserved in either of these situations because of friction and topography near the surface and poleward momentum fluxes by midlatitude waves (baroclinic eddies) in the upper troposphere.

The poleward momentum fluxes by baroclinic eddies from the tropical to midlatitude upper troposphere help to weaken the strength of the subtropical jets and drive the Ferrel cells and mid-latitude (eddy-driven) jet streams in each hemisphere. The eddy-driven jet streams are characterized by west-to-east winds throughout the depth of the troposphere in the midlatitudes of both hemispheres (Fig. 2), which are distinct from the subtropical jets that are only characterized by strong west-to-east flow in the upper troposphere. The Ferrel cell and eddy-driven jet stream are stronger in the SH, consistent with the much stronger zonal-mean storm track over SH midlatitudes. The eddy-driven jet stream is also much more distinct and separated from the subtropical jet in the SH, except during the summer season. The Ferrel cell and eddy-driven jet stream are weaker in the NH and display a more pronounced seasonal cycle, becoming much weaker in summer as the equator-to-pole meridional temperature gradient decreases.

In the stratosphere, zonal-mean zonal winds are characterized by easterlies in the summer hemisphere and westerlies in the winter hemisphere. The seasonal reversal of the winds is consistent with the seasonal reversal of the meridional temperature gradient, with solar-induced ozone heating creating a warmer pole during summer and a colder pole during winter (when no sunlight is present). The winter stratospheric westerlies (stratospheric polar vortex) are stronger in the SH (Fig. 2c). Planetary-scale Rossby waves, which are forced by topography and land-sea contrast, are more prominent in the NH, and these waves propagate upward into the stratosphere during winter where they transport heat to the pole and correspondingly weaken the stratospheric polar vortex. Small-scale orographic gravity waves, which are also more prominent in the NH, similarly weaken the stratospheric polar vortex.

The latest generation of climate models capture the climatological characteristics of the observed meridional overturning circulation and zonal-mean zonal wind reasonably well. However, there are several notable biases (see colored shading in Figs. 1 and 2). First, the midlatitude eddy-driven jet stream in the SH is displaced equatorward compared to observations. While this bias has improved in CMIP6 models compared to previous generations of models, it still persists in many models, particularly during winter months (Fig. 2c; Bracegirdle et al., 2020; Curtis et al., 2020). In summer months, SH midlatitude jet speeds tend to be too strong (Fig. 2b; Simpson et al., 2020). In the NH, the position of the eddy-driven jet stream reflects competing biases from the Atlantic and Pacific sectors, but in the zonal mean is too equatorward in winter and too poleward in summer (Simpson et al., 2020) and too strong in winter months (Fig. 2b). Overall, near-surface easterlies in the tropics and westerlies in the midlatitudes are generally overestimated in global climate models, potentially due to an improper parameterization of low-level drag by unresolved mountains (Pithan et al., 2016). In the upper troposphere and lower stratosphere, models generally have a westerly bias on the equatorward and upper flank of the subtropical jet, a westerly bias on the equatorward flank of the stratospheric polar vortex, and an easterly bias in the equatorial lower stratosphere (see also Fig. 4 of Pithan et al., 2016). The easterly bias in the equatorial lower stratosphere reflects, at least in part, model biases in the representation of the quasi-biennial oscillation (QBO) (see discussion below in next section).

In terms of the meridional overturning circulation, model biases are more challenging to characterize, given that there can be substantial spread in climatological values among reanalysis products. One of the clearest biases in CMIP6 models is an equatorward extension of the NH cell (positive anomalies near Equator in Fig. 1; Hur et al., 2022), consistent with excess precipitation in the South Pacific Convergence Zone, which is commonly referred to as the double-ITCZ bias (Tian and Dong, 2020). There is no systematic bias in the Hadley cell extent in CMIP6 models, and there is a slight tendency for the Hadley cells to be too strong, although with large inter-model spread (Simpson et al., 2020). The one exception is the annual-mean SH Hadley cell, which is biased weak (Fig. 1a). The inter-model spread in the strength of the Hadley cell has been related to extratropical wave driving (Caballero, 2008; Hur et al., 2022). Finally, the wintertime Ferrel cell is narrower on the poleward flank, consistent with the equatorward wintertime midlatitude jet bias seen in Fig. 2.

Internal variability

The zonal-mean atmospheric circulation is strongly affected by internal climate variability across a variety of timescales, ranging from weekly to multi-decadal. The leading mode of variability in the extratropical circulation of each hemisphere is an annular mode, which reflects a meridional displacement in the latitude of the eddy-driven jet stream with an e-folding timescale of approximately 10 days. In the SH, the timescale of the annular mode (SAM) slightly lengthens in the late spring-early summer when variability in the seasonal breakdown of the stratospheric polar vortex (i.e., the seasonal reversal from westerly to easterly winds) imparts a signal on the SAM (Baldwin et al., 2003; Byrne and Shepherd, 2018). Models generally capture the structure and magnitude of the SAM, although with an equatorward bias in the mean position (consistent with the equatorward-biased jet noted in the previous section) and some differences in regional structure (Simpson et al., 2020). The most notable bias is that variability in the SH eddy-driven jet latitude is often too persistent in climate models, particularly in summer months. The observed lengthening of the SAM timescale in late spring-early summer also extends too far into the summer (January and February) in models compared to observations (Gerber et al., 2010). The SAM timescale bias has somewhat improved in CMIP6 models and may be tied to the improvement in the equatorward jet latitude bias (Bracegirdle et al., 2020).

Models also generally capture the structure of the annular mode in the NH (NAM), although with biases in the mean position (consistent with the biases in the mean jet latitude discussed in the previous section) and some differences in regional structure (Simpson et al., 2020). In particular, the contribution of jet variability over the North Pacific sector to the NAM is overemphasized in models compared to observations (Coburn and Pryor, 2021; Lee and Polvani, 2024). As with the SAM, models struggle to properly capture the timescales of jet variability in the NH. During winter months, the observed NAM timescale lengthens, as variability in the stratospheric polar vortex driven by planetary waves imparts enhanced memory to the NAM (Baldwin et al., 2003). Models with lower tops (within the stratosphere) struggle to properly capture stratospheric variability (Lee and Black, 2015), which some studies have shown to impact the timescale of the tropospheric NAM (Charlton-Perez et al., 2013). Proper representation of the coupling between the stratosphere and troposphere is likely necessary to correctly model the timescales of Northern Hemisphere jet variability in winter. More generally, models particularly struggle with a "signal-to-noise" paradox in the North Atlantic sector (Scaife and Smith, 2018), often containing similar amounts of variance to observations but that is much more noisy (less predictable) than in observations. This "signal-to-noise paradox" impacts the behavior of the meridional jet shifts in the North Atlantic sector (North Atlantic Oscillation), which is closely correlated with the NAM.

Week-to-week variability in the stratospheric circulation is dominated by the upward fluxes of planetary wave activity from the troposphere during seasons when the mean flow is westerly. These waves can displace the stratospheric polar vortex from the pole or even split the vortex, creating a rapid warming of the polar stratosphere on the timescale of days (sudden stratospheric warming) and a reversal of the zonal-mean zonal winds in the polar stratosphere. Due to the prevalence of planetary wave activity, sudden stratospheric warmings are much more common in the NH, generally occurring in 6 out of 10 years in the Arctic stratosphere (Charlton and Polvani, 2007). Climate models vary widely in their representation of the frequency of Arctic sudden stratospheric warmings, with some models exhibiting almost no warmings and others showing warmings more than once per year, although the average model bias is for too few warmings (Wu and Reichler, 2020). Correctly modeling the frequency of sudden stratospheric

warmings depends on an accurate representation of the strength of the polar vortex and the upward propagating planetary and gravity waves from the troposphere, which requires a higher model top, accurate modeling of the mean-state stratospheric circulation, and enhanced vertical resolution in the stratosphere (Seviour et al., 2016; Wu and Reichler, 2020).

On interannual timescales, the dominant mode of variability in Earth's climate system is the El Niño-Southern Oscillation (ENSO). During the El Niño phase, which occurs irregularly every 2–7 years, sea surface temperature (SST) in the eastern tropical Pacific Ocean becomes anomalously warm and is associated with a series of changes in the tropical atmospheric circulation with teleconnections to the extratropics. For the zonal-mean atmospheric circulation, El Niño is associated with a strengthening and equatorward contraction of the Hadley cell, strengthening of the subtropical jet, and equatorward shift of the eddy-driven jet (L'Heureux and Thompson, 2006; Lu et al., 2008; Seager et al., 2003). The equatorward contraction of the circulation is hypothesized to be closely related to the narrowness of the tropical heating anomalies associated with El Niño (Sun et al., 2013; Tandon et al., 2013). The La Niña phase of ENSO, marked by anomalously cool SSTs in the eastern tropical Pacific, is associated with the opposite effects (i.e., a poleward shifted and weaker circulation). ENSO SST anomalies are largest in boreal winter (December–February, or DJF), and the effects of ENSO on the zonal-mean atmospheric circulation are also largest during this season.

The ability of models to represent the impacts of ENSO on the zonal-mean circulation depends on the ability of the models to (1) simulate the ENSO events themselves and (2) simulate the circulation response to an ENSO event. While there is large inter-model variance, models on average simulate ENSO events that are qualitatively similar to observations, although with some notable biases. Models reasonably capture the amplitude of observed ENSO events during boreal winter (although individual models vary widely), but underestimate the observed suppression of ENSO variance in boreal spring (Eyring et al., 2021). Additionally, observed La Niña events are generally longer in duration than El Niño events, while models depict El Niño and La Niña events of similar duration. These biases will consequently impact models' representation of interannual variability in the zonal-mean zonal wind and Hadley circulation.

Most models well capture the circulation response to ENSO (Lu et al., 2008). As in observations, climate models show a strengthening and equatorward contraction of the Hadley cell, strengthening of the subtropical jet, and equatorward shift of the eddy-driven jet with an El Niño event. However, Lim et al. (2016) have shown that an earlier generation of models underestimated the impacts of ENSO on the SH extratropical circulation (SAM) during DJF. Although the cause of this bias was not investigated, it is likely that model bias in the SST anomalies associated with ENSO impact teleconnections to the extratropics. For example, models generally underestimate the meridional width of the El Niño SST anomalies along the Equator in the eastern tropical Pacific Ocean (Zhang and Jin, 2012). Underestimated teleconnections to the extratropics may also be associated with the underestimation and too-far westward extension of tropical precipitation anomalies associated with ENSO, which are related to mean-state SST biases in models (Fang et al., 2024).

More generally, interannual connections between the tropical and extratropical tropospheric circulations are also affected by model mean-state biases. Both observations and models show a strong correlation between the latitudes of the eddy-driven jet and Hadley cell edge in the SH during DJF, with the eddy-driven jet shifting poleward by 1.5–2 degrees latitude for every 1 degree latitude poleward shift in the Hadley cell edge (Kang and Polvani, 2011). However, the amplitude and robustness of this relationship varies across models, with the weakest values in models where the jet and Hadley cell edge are farthest apart in their mean-state climatology (Kidston et al., 2013; Waugh et al., 2018). Climatologically, the Hadley cell edge and eddy-driven jet are closest to one another during summer (DJF) in the SH, but become much farther apart in winter (June–August, or JJA). Consequently, in both observations and models, interannual variability in the SH Hadley cell edge and eddy-driven jet latitude are no longer robustly correlated in JJA. Correlations between the Hadley cell edge and eddy-driven jet latitude are moderate in the NH during all seasons (Waugh et al., 2018). While variability in the strength of the subtropical jet is negatively correlated with the Hadley cell edge and eddy-driven jet positions on interannual timescales (consistent with the ENSO relationships discussed above), variability in the location of the subtropical jet is very poorly correlated with both the Hadley cell and eddy-driven jet (Menzel et al., 2019).

At stratospheric levels, the quasi-biennial oscillation (QBO) dominates interannual variability. The QBO refers to alternating westerly and easterly zonal-mean zonal wind anomalies that descend through the equatorial stratosphere with a period of approximately 28 months. The QBO is driven by momentum deposited by upward propagating gravity, Kelvin, and mixed Rossby-gravity waves (Baldwin et al., 2001). Early generation climate models did not include a QBO, but approximately half of CMIP6 models now include a QBO (Richter et al., 2020). The models generally capture the observed period of the QBO (with some exceptions), as well as its amplitude and meridional extent in the mid-stratosphere. However, models substantially underestimate the QBO amplitude in the lower stratosphere, such that the QBO tends to be shifted upward in models compared to observations (Bushell et al., 2022; Richter et al., 2020). Proposed causes for model biases in the QBO include inadequate vertical resolution, zonal mean zonal wind biases, and improper resolved wave forcing by Kelvin and mixed Rossby-gravity waves (Bushell et al., 2022; Holt et al., 2022; Richter et al., 2020). Models generally rely on the tuning of parameterized non-orographic gravity wave forcing to produce a QBO that is realistic compared to observations. A model's fidelity at simulating the QBO not only affects interannual zonal-mean zonal wind variability in the tropical stratosphere, but also in the extratropical stratosphere. The QBO helps to modulate the propagation of planetary waves into the extratropical stratosphere during winter, such that the stratospheric polar vortex is stronger and sudden stratospheric warmings are less likely during the westerly phase of the QBO (Holton and Tan, 1980). However, this effect is consistently too weak in models, which may be a consequence of the upward shift bias in their representation of the QBO (Anstey et al., 2022).

On decadal and multi-decadal timescales, variability in the Pacific and Atlantic Oceans can impact the zonal-mean zonal wind and Hadley circulation. In the Pacific, multi-decadal variability (Pacific Decadal Variability, or PDV) is characterized by SST anomalies of one sign in the eastern tropical Pacific Ocean and along the west coast of North America, and SST anomalies of opposite sign in the western north and south Pacific Oceans (Henley et al., 2015). The positive phase of PDV, marked by positive SST anomalies along the Equator in the eastern tropical Pacific similar to an El Niño event, is associated with similar impacts on the zonal-mean atmospheric circulation to an El Niño event. Periods of multi-decadal poleward circulation shifts occur in pre-industrial runs of global climate models (i.e., hundreds of years of simulation with no anthropogenic forcing) and are associated with SST trends that resemble the negative (La Niña-like) phase of PDV (Allen and Kovilakam, 2017; Grise et al., 2019). As such, shifts in the phase of PDV can impart multi-decadal trends in the atmospheric circulation, which are due to internal variability in the climate system and not climate change. For example, the shift from the positive to negative PDV phase in the late 1990s contributed to a poleward shift in the edges of the Hadley circulation, likely compounding the expected expansion of the Hadley circulation due to climate change (see next section).

The latest generation of models has improved in their representation of the spatial structure and magnitude of PDV compared to previous generations, but remains deficient in the simulation of PDV in several regards (Eyring et al., 2021). In particular, models tend to underestimate the duration of PDV phases, showing greater interannual versus decadal variance compared to observations (Henley, 2017; Kociuba and Power, 2015). Any biases in model representation of PDV will consequently impact decadal variability in the zonal-mean zonal wind and Hadley circulation in models. However, assessing the representation of PDV in models is challenging, given the limited number of realizations of PDV captured in observations.

In the Atlantic, multi-decadal variability (Atlantic Multidecadal Variability, or AMV) is characterized by a basin-wide warming or cooling in the North Atlantic basin. Possible drivers of AMV include the Atlantic Meridional Overturning Circulation and decadal variability in the North Atlantic jet stream. Multi-annual persistence of a certain phase of the NAO during winter can impact AMV, but the AMV itself may in turn feed back on the atmosphere and drive a shift in phase of the winter NAO (Gastineau and Frankignoul, 2015; Peings et al., 2016; Woollings et al., 2015). In particular, a warm AMV phase may help to drive the negative phase of the NAO/NAM during winter in observations and in some climate models. Similar to PDV, shifts in the phase of AMV have the potential to impart multi-decadal trends in the atmospheric circulation, which are due to internal variability in the climate system and not climate change.

Assessing the representation of AMV in climate models is challenging due to the limited number of realizations captured in observations and the fact that anthropogenic forcing has likely contributed to recent AMV changes during the observational record. CMIP6 models appear to overestimate decadal SST variance in the North Atlantic and underestimate it in the tropical Atlantic, whereas the previous generation of models tended to underestimate the duration and magnitude of AMV (Eyring et al., 2021). Models generally underestimate multi-decadal-scale variance in the NAM/NAO compared to observations (Bonnet et al., 2024; Bracegirdle et al., 2018; Simpson et al., 2018; Wang et al., 2017). Observed multi-decadal variability in North Atlantic zonal wind peaks in late winter (February and March), possibly due to AMV, whereas models do not show this peak and have similar multi-decadal variance during all months, consistent with white noise (Simpson et al., 2018).

Historical trends

The zonal-mean atmospheric circulation has experienced notable trends in recent decades, and climate models differ in their ability to replicate these trends. However, one must be cautious in directly comparing trends from observations with those from climate models. As noted in the previous section, internal atmospheric variability and coupled atmosphere-ocean variability can produce multi-decadal trends in the atmospheric circulation, which are difficult to distinguish from trends due to external forcing (such as changes in atmospheric composition or solar forcing), particularly when the internal variability acts in the same direction as the forcing. In recent decades, observed historical trends comprise trends from internal variability in the climate system and long-term forced trends due to increasing greenhouse gases, stratospheric ozone depletion, and changes in atmospheric aerosol concentrations. In contrast, historical simulations from climate models are forced by best estimates of observed changes in atmospheric composition, solar forcing, and land use change and thus, on average, only simulate the forced component of the trend. Therefore, it is necessary to compare observed circulation trends with trends from individual model runs (which encompass a model's own internal variability plus the trend from external forcing) instead of to an average of model runs (which, by definition, averages out internal variability and only isolates the forced component of the trend).

This section focuses on circulation trends over the period 1979–2014. 1979 marks the beginning of global satellite data coverage, which is assimilated into reanalysis data sets that provide the best estimate of long-term global changes in the atmospheric circulation. However, even still, circulation trends from reanalysis products vary greatly, and it is wise to assess the robustness of trends across multiple reanalysis data sets. 2014 marks the end of the CMIP6 simulations forced by historical forcings.

One of the most notable atmospheric circulation trends observed since 1979 has been the poleward expansion of Earth's Hadley circulation. Some early estimates of this expansion exceeded 1° latitude per decade (Johanson and Fu, 2009; Seidel et al., 2008), but many of these earlier reported values were based on older generation reanalysis products and metrics for measuring the Hadley cell edge that were flawed and/or not well constrained by surface observations. When the Hadley cell edge is defined using appropriate metrics and using more modern reanalyses, observed rates of Hadley cell expansion are more consistent with those from climate models over the historical period ($0.2^{\circ}-0.4^{\circ}$ per decade) (Fig. 3; Grise et al., 2019). Models indicate that increasing greenhouse gases

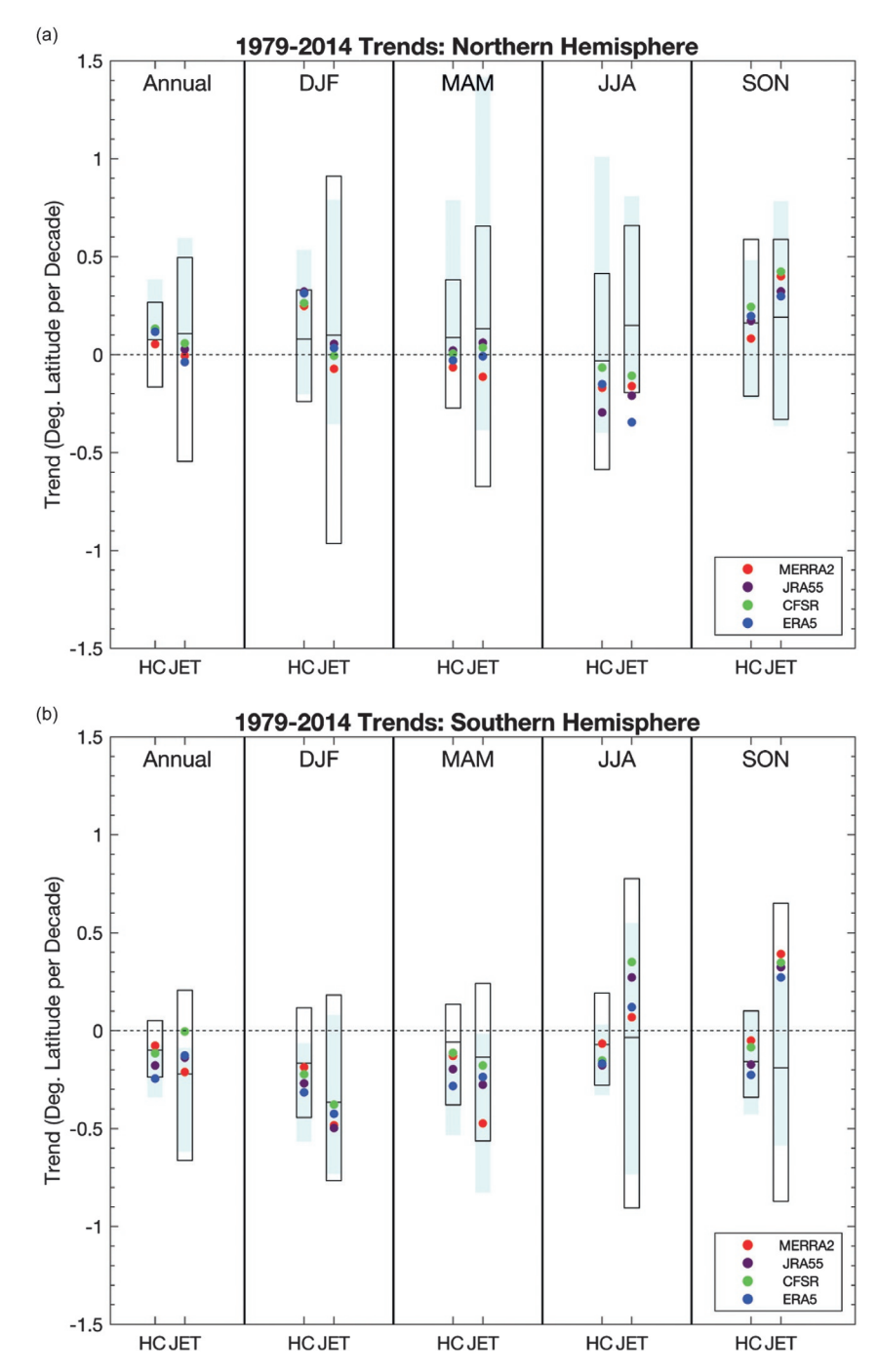


Fig. 3 1979–2014 trends in the position of the Hadley cell (HC) edge and midlatitude eddy-driven jet in both hemispheres for (colored symbols) four reanalysis products, (black box) range for trends from the historical runs of 20 CMIP6 models (horizontal line: multi-model mean), and (light blue box) range for trends from the AMIP (prescribed observed SST) runs of 20 CMIP6 models. Trends are shown for the annual mean and the four seasonal means (December–February, March–May, June–August, and September–November). Following Grise et al. (2018), the Hadley cell edge latitude is calculated using the zero crossing of the zonal-mean zonal surface wind in the subtropics, and the jet latitude is calculated using the maximum of the 850-hPa zonal-mean zonal wind field (see also Adam et al., 2018).

should drive larger expansion in the SH (Watt-Meyer et al., 2019), which is also seen to a lesser extent in runs forced with all historical forcings (Fig. 3, horizontal black lines). However, observed rates of expansion are comparable between the two hemispheres (Grise and Davis, 2020). If climate models are forced with observed sea surface temperatures in addition to atmospheric composition changes, then the models can produce larger and more comparable rates of expansion in the two hemispheres (Fig. 3, light blue bars). This points to the important role of multi-decadal SST variability (such as the change in phase of PDV from positive to negative in the late 1990s) in driving the observed circulation trends, particularly in the NH.

Given the close connection between the eddy-driven jet latitude and Hadley cell edge noted above during some seasons, it is not surprising that poleward jet shifts have likewise been documented in recent decades, particularly during DJF, in both the SH (Fig. 3b) and the NH (if the end point for the trend is extended through the early 2020s; Woollings et al., 2023). In the SH, the magnitude of the observed eddy-driven jet shift is largest during DJF, which is consistent with expectations from climate models. Climate models indicate that the magnitude of the trend over the late 20th century during DJF would have been very unlikely without the presence of anthropogenic forcing, reflecting the combined influence of increasing greenhouse gases and stratospheric ozone depletion (Lee and Feldstein, 2013; Waugh et al., 2015). Stratospheric ozone depletion makes the Antarctic stratosphere anomalously cold during the spring season and strengthens the stratospheric polar vortex, which couples down to the troposphere as a positive SAM response (poleward circulation shift) during summer months (Thompson and Solomon, 2002). Increasing greenhouse gases raise global-mean surface temperature, which enhances the water vapor concentration in Earth's atmosphere. The enhanced water vapor concentration allows for enhanced latent heat release in the mid-to-upper troposphere, stabilizing the subtropical atmosphere to baroclinic wave activity and thus allowing the Hadley cell to extend further poleward (Chemke and Polvani, 2019a). Given the close connection between the Hadley cell edge and eddy-driven jet in the SH during DJF (see previous section), the jet also shifts poleward with the Hadley cell edge in response to increasing greenhouse gases. In the early 21st century, as stratospheric ozone depletion has stabilized and is beginning to recover, climate models indicate that the poleward jet shift associated with increasing greenhouse gases will begin to be compensated by an equatorward jet shift associated with the recovering ozone hole, slowing the overall rate of expansion of the circulation (Barnes et al., 2014). Observational evidence is beginning to show evidence of a slowdown or pause in the SH circulation trends during DJF (Banerjee et al., 2020). It is worth noting that climatological biases in the location of the SH eddy-driven jet may impact a model's projected trends in response to forcing (Kidston and Gerber, 2010; Son et al., 2010), particularly during the JJA season (Simpson and Polvani, 2016).

In the NH, the circulation shift in a warming climate is thought to reflect two competing factors. First, as in the SH, enhanced latent heat release in the mid-to-upper troposphere stabilizes the subtropical atmosphere and enhances the meridional temperature gradient between the tropical upper troposphere and polar lower stratosphere, contributing to a poleward circulation shift. However, in the NH, amplified surface warming in the Arctic reduces the meridional temperature gradient in the lower troposphere, contributing to an equatorward circulation shift that may counteract or damp the poleward circulation shift driven from upper levels (Barnes and Screen, 2015). In recent decades, the observed NH poleward circulation shift is largest in winter (DJF) and fall (September–November, or SON), whereas climate models project the largest poleward shift during SON in response to historical forcing (Fig. 3a). While the observed wintertime trends could be associated with the recent phase change in the PDO (Fig. 3a, light blue bars), the observed fall trends suggest the role of anthropogenic forcing (Grise et al., 2018). Climate models forced only by increasing greenhouse gases indicate that poleward Hadley cell expansion in the NH is substantially larger in SON, comparable to that projected for the SH (Watt-Meyer et al., 2019).

In contrast to the SH, historical trends in Arctic polar stratospheric temperatures and zonal wind are weaker, with a less clear role in NH tropospheric circulation trends. As a result of its warmer temperatures, the extent of ozone depletion in the Arctic stratosphere is much less than that in the Antarctic. However, one notable feature of the historical NH stratospheric circulation is the relatively strong polar vortex that persisted during the 1990s. A consequence of this is that the 1990s saw just 2 sudden stratospheric warming (SSW) events, in which the westerly polar vortex breaks down in winter, while the 1980s and 2000s each had 9 (Butler et al., 2017). This SSW 'drought' imprints on surface variability, in particular, being related to a reduced frequency of negative (i.e., equatorward shift) NAM/NAO events during the period (Domeisen, 2019). There is no modeling evidence that this decadal variability is a result of external forcing, though it should be noted that models vary widely in their representation of NH polar vortex variability and trends

In terms of the strength of the Hadley cells, reanalysis products generally indicate a strengthening in recent decades (Zaplotnik et al., 2022), which is in contrast to the general weakening trend predicted by climate models for Hadley cell strength in the NH (Chemke and Polvani, 2019b). A weakening of the Hadley cell is anticipated as the overall tropical circulation is expected to slow down to close the global energy balance, as global precipitation increases at a slower rate than water vapor with warming (Held and Soden, 2006). However, the recent reanalysis trends likely reflect biases in latent heating in reanalysis (Chemke and Polvani, 2019b). When sea level pressure observations are used to estimate recent observed NH Hadley cell strength trends, the observed trends show weakening, more in line with those expected from climate models (Chemke and Yuval, 2023).

In terms of the strength of the jet streams, observations show a strengthening, upward, and poleward shift of the zonal-mean zonal wind in both hemispheres during the DJF season since 1979; trends in other seasons are less significant (Woollings et al., 2023). These trends during the DJF season closely correspond to those predicted by climate models forced with historical forcing. As noted earlier, enhanced warming in the tropical upper troposphere is a key signature of climate warming, which increases the equator-to-pole temperature gradient and strengthens the shear of the upper tropospheric zonal wind according to thermal wind balance. In the SH, the equator-to-pole temperature gradient is further enhanced by the thermal response to depleted stratospheric ozone.

During the JJA season, observations have shown a weakening of the NH eddy-driven jet since 1979, which is consistent with a weakening of the equator-to-pole temperature gradient during this season (Coumou et al., 2015). The historical simulations of CMIP6 models are able to capture this weakening and suggest that it is a result of both anthropogenic aerosol and greenhouse gas forcing (Kang et al., 2024). Greenhouse gases contribute to enhanced warming at Arctic latitudes, weakening the meridional temperature gradient. Decreased anthropogenic aerosols (and enhanced solar absorption) at higher latitudes and increased anthropogenic aerosols (and reduced solar absorption) at lower latitudes of the NH likewise have weakened the meridional temperature gradient.

Conclusion

Overall, the latest generation of global climate models well capture the climatology, variability, and recent observed trends in the zonal-mean atmospheric circulation, including the Hadley circulation and subtropical and eddy-driven jet streams. Biases in mean-state flow have been improved in CMIP6 models, but certain persistent biases remain. Representation of variability in the zonal-mean atmospheric circulation by climate models is affected by how well models capture modes of internal climate variability. Deficiencies in models capturing multi-decadal variability in the ocean likely imprint on inadequate decadal variability in the atmospheric circulation. Climate models now generally capture many of the circulation trends observed over the late 20th and early 21st centuries, due to improvements in models, methodologies, and reanalysis data sets. Comparing observed and model trends over 30–40 periods is complicated by the large signal of internal variability on these timescales. As the observational record lengthens, it is expected that more forced circulation trends will begin emerging, allowing for an assessment of the accuracy of models in simulating forced circulation changes due to anthropogenic forcing (Shaw et al., 2024). However, as shown in this chapter, early results indicate that models are a skillful tool at representing and understanding the cause behind forced circulation changes in the climate system.

References

Adam O, Grise K, Staten P, Simpson I, Davis S, Davis N, Waugh D, Birner T, and Ming A (2018) The TropD software package (v1): Standardized methods for calculating tropical-width diagnostics. *Geoscientific Model Development* 11: 4339–4357.

Allen R and Kovilakam M (2017) The role of natural climate variability in recent tropical expansion. Journal of Climate 30: 6329-6350.

Anstey J, Simpson I, Richter J, Naoe H, Taguchi M, Serva F, Gray L, Butchart N, Hamilton K, Osprey S, and Bellprat 0 (2022) Teleconnections of the quasi-biennial oscillation in a multi-model ensemble of QBO-resolving models. *Quarterly Journal of the Royal Meteorological Society* 148: 1568–1592.

Baldwin M, Gray L, Dunkerton T, Hamilton K, Haynes P, Randel W, Holton J, Alexander M, Hirota I, Horinouchi T, Jones D, Kinnersley J, Marquardt C, Sato K, and Takahashi M (2001) The quasi-biennial oscillation. *Reviews of Geophysics* 39: 179–229.

Baldwin M, Stephenson D, Thompson D, Dunkerton T, Charlton A, and O'Neill A (2003) Stratospheric memory and skill of extended-range weather forecasts. *Science* 301: 636–640. Banerjee A, Fyfe J, Polvani L, Waugh D, and Chang K-L (2020) A pause in Southern Hemisphere circulation trends due to the Montreal Protocol. *Nature* 579: 544–548.

Barnes E and Screen J (2015) The impact of Arctic warming on the midlatitude jet-stream: Can it? Has it? Will it? WIREs Climate Change 6: 277–286.

Barnes E, Barnes N, and Polvani L (2014) Delayed southern hemisphere climate change induced by stratospheric ozone recovery, as projected by the CMIP5 models. *Journal of Climate* 27: 852–867.

Bonnet R, McKenna C, and Maycock A (2024) Model spread in multidecadal North Atlantic Oscillation variability connected to stratosphere—troposphere coupling. *Weather and Climate Dynamics* 5: 913–926.

Bracegirdle T, Lu H, Eade R, and Woollings T (2018) Do CMIP5 models reproduce observed low-frequency North Atlantic jet variability? *Geophysical Research Letters* 45: 7204–7212. Bracegirdle T, Holmes C, Hosking J, Marshall G, Osman M, Patterson M, and Rackow T (2020) Improvements in circumpolar Southern Hemisphere extratropical atmospheric circulation in CMIP6 compared to CMIP5. Earth and Space. *Science* 7: e2019EA001065.

Bushell A, Anstey J, Butchart N, Kawatani Y, Osprey S, Richter J, Serva F, Braesicke P, Cagnazzo C, Chen C-C, Chun H-Y, Garcia R, Gray L, Hamilton K, Kerzenmacher T, Kim Y-H, Lott F, McLandress C, Naoe H, Scinocca J, Smith A, Stockdale T, Versick S, Watanabe S, Yoshida K, and Yukimoto S (2022) Evaluation of the Quasi-Biennial Oscillation in global climate models for the SPARC QBO-initiative. *Quarterly Journal of the Royal Meteorological Society* 148: 1459–1489.

Butler A, Sjoberg J, Seidel D, and Rosenlof K (2017) A sudden stratospheric warming compendium. Earth System Science Data 9: 63-76.

Byrne N and Shepherd T (2018) Seasonal persistence of circulation anomalies in the southern hemisphere stratosphere and its implications for the troposphere. *Journal of Climate* 31: 3467–3483.

Caballero R (2008) Hadley cell bias in climate models linked to extratropical eddy stress. *Geophysical Research Letters* 35: L18709.

Charlton A and Polvani L (2007) A new look at stratospheric sudden warmings. Part I: Climatology and modeling benchmarks. Journal of Climate 20: 449-469.

Charlton-Perez A, Baldwin M, Birner T, Black R, Butler A, Calvo N, Davis N, Gerber E, Gillett N, Hardiman S, Kim J, Krüger K, Lee Y-Y, Manzini E, McDaniel B, Polvani L, Reichler T, Shaw T, Sigmond M, Son S-W, Toohey M, Wilcox L, Yoden S, Christiansen B, Lott F, Shindell D, Yukimoto S, and Watanabe S (2013) On the lack of stratospheric dynamical variability in low-top versions of the CMIP5 models. *Journal of Geophysical Research – Atmospheres* 118: 2494–2505.

Chemke R and Polvani L (2019a) Exploiting the abrupt 4×CO2 scenario to elucidate tropical expansion mechanisms. Journal of Climate 32: 859-875.

Chemke R and Polvani LM (2019b) Opposite tropical circulation trends in climate models and in reanalyses. Nature Geoscience 12: 528-532.

Chemke R and Yuval J (2023) Human-induced weakening of the Northern Hemisphere tropical circulation. Nature 617: 529-532.

Coburn J and Pryor S (2021) Differential credibility of climate modes in CMIP6. Journal of Climate 34: 8145-8164.

Coumou D, Lehmann J, and Beckmann J (2015) The weakening summer circulation in the Northern Hemisphere mid-latitudes. Science 348: 324-327.

Curtis P, Ceppi P, and Zappa G (2020) Role of the mean state for the Southern Hemispheric jet stream response to CO₂ forcing in CMIP6 models. *Environmental Research Letters* 15: 064011

Dima I and Wallace J (2003) On the seasonality of the Hadley cell. Journal of the Atmospheric Sciences 60: 1522-1527.

Domeisen D (2019) Estimating the frequency of sudden stratospheric warming events from surface observations of the North Atlantic Oscillation. *Journal of Geophysical Research* 124: 3180–3194.

Eyring V, Gillett N, Achuta Rao K, Barimalala R, Barreiro Parrillo M, Bellouin N, Cassou C, Durack P, Kosaka Y, McGregor S, Min S, Morgenstern O, and Sun Y (2021) Human influence on the climate system. In: Masson-Delmotte V, Zhai P, Pirani A, Connors S, Péan C, Berger S, and Zhou B (eds.) , Climate Change 2021: The Physical Science Basis. Contribution of Working Group I to the Sixth Assessment Report of the Intergovernmental Panel on Climate Change, pp. 423–552. Cambridge, United Kingdom and New York, NY, USA: Cambridge University Press.

Fang Y, Screen J, Hu X, Lin S, Williams N, and Yang S (2024) CMIP6 models underestimate ENSO teleconnections in the Southern Hemisphere. *Geophysical Research Letters* 51. e2024GL110738.

Gastineau G and Frankignoul C (2015) Influence of the North Atlantic SST variability on the atmospheric circulation during the twentieth century. *Journal of Climate* 28: 1396–1416. Gerber E, Baldwin M, Akiyoshi H, Austin J, Bekki S, Braesicke P, Butchart N, Chipperfield M, Dameris M, Dhomse S, Frith S, Garcia R, Garny H, Gettelman A, Hardiman S, Karpechko A, Marchand M, Morgenstern O, Nielsen J, Pawson S, Peter T, Plummer D, Pyle J, Rozanov E, Scinocca J, Shepherd T, and Smale D (2010) Stratosphere-troposphere coupling and annular mode variability in chemistry-climate models. *Journal of Geophysical Research* 115: D00M06.

Grise K and Davis S (2020) Hadley cell expansion in CMIP6 models. Atmospheric Chemistry and Physics 20: 5249-5268.

Grise K, Davis S, Staten P, and Adam O (2018) Regional and seasonal characteristics of the recent expansion of the tropics. Journal of Climate 31: 6839-6856.

Grise K, Davis S, Simpson I, Waugh D, Fu Q, Allen R, Rosenlof K, Ummenhofer C, Karnauskas K, Maycock A, Quan X, Birner T, and Staten P (2019) Recent tropical expansion: Natural variability or forced response? *Journal of Climate* 32: 1551–1571.

Held I and Soden B (2006) Robust responses of the hydrological cycle to global warming. Journal of Climate 19: 5686-5699.

Henley B (2017) Pacific decadal climate variability: Indices, patterns and tropical-extratropical interactions. Global and Planetary Change 155: 42-55.

Henley B, Gergis J, Karoly D, Power S, Kennedy J, and Folland C (2015) A tripole index for the interdecadal pacific oscillation. Climate Dynamics 45: 3077–3090.

Holt L, Lott F, Garcia R, Kiladis G, Cheng Y-M, Anstey J, Braesicke P, Bushell A, Butchart N, Cagnazzo C, Chen C-C, Chun H-Y, Kawatani Y, Kerzenmacher T, Kim Y-H, McLandress C, Naoe H, Osprey S, Richter J, Scaife A, Scinocca J, Serva F, Versick S, Watanabe S, Yoshida K, and Yukimoto S (2022) An evaluation of tropical waves and wave forcing of the QBO in the QBO in models. *Quarterly Journal of the Royal Meteorological Society* 148: 1541–1567.

Holton J and Tan H (1980) The influence of the equatorial quasi-biennial oscillation on the global circulation at 50 mb. *Journal of the Atmospheric Sciences* 37: 2200–2208. Hur I, Kim M, Kwak K, Sung H, Byun Y-H, Song H, and Yoo C (2022) Hadley circulation in the present and future climate simulations of the K-ACE model. *Asia-Pacific Journal of*

Atmospheric Sciences 58: 353–363.

Johanson C and Fu Q (2009) Hadley cell widening: Model simulations versus observations. *Journal of Climate* 22: 2713–2725.

Kang S and Polvani L (2011) The interannual relationship between the latitude of the Eddy-driven jet and the edge of the Hadley cell. Journal of Climate 24: 563-568.

Kang J, Shaw T, and Sun L (2024) Anthropogenic aerosols have significantly weakened the regional summertime circulation in the Northern Hemisphere during the satellite era. *AGU Advances* 5: e2024AV001318.

Kidston J and Gerber E (2010) Intermodel variability of the poleward shift of the austral jet stream in the CMIP3 integrations linked to biases in 20th century climatology. *Geophysical Research Letters* 37: L09708.

Kidston J, Cairns C, and Paga P (2013) Variability in the width of the tropics and the annular modes. Geophysical Research Letters 40: 2328–2332.

Kociuba G and Power S (2015) Inability of CMIP5 models to simulate recent strengthening of the walker circulation: Implications for projections, Journal of Climate 28: 20–35.

L'Heureux M and Thompson D (2006) Observed relationships between the El Niño-Southern oscillation and the extratropical zonal-mean circulation. Journal of Climate 19: 276–287.

Lee Y and Black R (2015) The structure and dynamics of the stratospheric northern annular mode in CMIP5 simulations. Journal of Climate 28: 86–107.

Lee S and Feldstein S (2013) Detecting ozone- and greenhouse gas-driven wind trends with observational data. Science 339: 563-567.

Lee S and Polvani L (2024) Large model biases in the Pacific centre of the Northern Annular Mode due to exaggerated variability of the Aleutian Low. *Quarterly Journal of the Royal Meteorological Society* 150: 4478–4497.

Lim E-P, Hendon H, Arblaster J, Delage F, Nguyen H, Min S-K, and Wheeler M (2016) The impact of the southern annular mode on future changes in southern hemisphere rainfall. Geophysical Research Letters 43: 7160–7167.

Lu J, Chen G, and Frierson D (2008) Response of the zonal mean atmospheric circulation to El Niño versus global warming. Journal of Climate 21: 5835-5851.

Menzel M, Waugh D, and Grise K (2019) Disconnect between Hadley cell and subtropical jet variability and response to increased CO2. *Geophysical Research Letters* 46: 7045–7053. Peings Y, Simpkins G, and Magnusdottir G (2016) Multidecadal fluctuations of the North Atlantic Ocean and feedback on the winter climate in CMIP5 control simulations. *Journal of Geophysical Research – Atmospheres* 121: 2571–2592.

Pithan F, Shepherd T, Zappa G, and Sandu I (2016) Climate model biases in jet streams, blocking and storm tracks resulting from missing orographic drag. *Geophysical Research Letters* 43: 7231–7240.

Richter JH, Anstey J, Butchart N, Kawatani Y, Meehl G, Osprey S, and Simpson I (2020) Progress in simulating the quasi-biennial oscillation in CMIP models. *Journal of Geophysical Research – Atmospheres* 125. e2019JD032362.

Scaife A and Smith D (2018) A signal-to-noise paradox in climate science. npj Climate and Atmospheric Science 1: 28.

Schneider T, Bischoff T, and Haug G (2014) Migrations and dynamics of the intertropical convergence zone. Nature 513: 45-53.

Seager R, Harnik N, Kushnir Y, Robinson W, and Miller J (2003) Mechanisms of hemispherically symmetric climate variability. Journal of Climate 16: 2960-2978.

Seidel D, Fu Q, Randel W, and Reichler T (2008) Widening of the tropical belt in a changing climate. Nature Geoscience 1: 21-24.

Seviour W, Gray L, and Mitchell D (2016) Stratospheric polar vortex splits and displacements in the high-top CMIP5 climate models. *Journal of Geophysical Research – Atmospheres* 121: 1400–1413.

Shaw T, Arblaster J, Birner T, Butler A, Domeisen D, Garfinkel C, Garny H, Grise K, and Karpechko A (2024) Emerging climate change signals in atmospheric circulation. *AGU Advances* 5: e2024AV001297.

Simpson I and Polvani L (2016) Revisiting the relationship between jet position, forced response, and annular mode variability in the southern midlatitudes. *Geophysical Research Letters* 43: 2896–2903.

Simpson I, Deser C, McKinnon K, and Barnes E (2018) Modeled and observed multidecadal variability in the North Atlantic Jet stream and its connection to sea surface temperatures. Journal of Climate 31: 8313–8338.

Simpson I, Bacmeister J, Neale R, Hannay C, Gettelman A, Garcia R, Lauritzen P, Marsh D, Mills M, Medeiros B, and Richter J (2020) An evaluation of the large-scale atmospheric circulation and its variability in CESM2 and other CMIP models. *Journal of Geophysical Research – Atmospheres* 125: e2020JD032835.

Son S-W, Gerber E, Perlwitz J, Polvani L, Gillett N, Seo K-H, Eyring V, Shepherd T, Waugh D, Akiyoshi H, Austin J, Baumgaertner A, Bekki S, Braesicke P, Brühl C, Butchart N, Chipperfield M, Cugnet D, Dameris M, Dhomse S, Frith S, Garny H, Garcia R, Hardiman S, Jöckel P, Lamarque J, Mancini E, Marchand M, Michou M, Nakamura T, Morgenstern O, Pitari G, Plummer D, Pyle J, Rozanov E, Scinocca J, Shibata K, Smale D, Teyssèdre H, Tian W, and Yamashita Y (2010) Impact of stratospheric ozone on Southern Hemisphere circulation change: A multimodel assessment. *Journal of Geophysical Research* 115: D00M07.

Sun L, Chen G, and Lu J (2013) Sensitivities and mechanisms of the zonal mean atmospheric circulation response to tropical warming. *Journal of the Atmospheric Sciences* 70: 2487–2504.

Tandon N, Gerber E, Sobel A, and Polvani L (2013) Understanding Hadley cell expansion versus contraction: Insights from simplified models and implications for recent observations. Journal of Climate 26: 4304–4321.

Thompson D and Solomon S (2002) Interpretation of recent southern hemisphere climate change. Science 296: 895–899.

Tian B and Dong X (2020) The double-ITCZ Bias in CMIP3, CMIP5 and CMIP6 models based on annual mean precipitation. *Geophysical Research Letters* 47: e2020GL087232. Wang X, Li J, Sun C, and Liu T (2017) NAO and its relationship with the Northern Hemisphere mean surface temperature in CMIP5 simulations. *Journal of Geophysical Research – Atmospheres* 122: 4202–4227.

Watt-Meyer O, Frierson D, and Fu Q (2019) Hemispheric asymmetry of tropical expansion under CO₂ forcing. Geophysical Research Letters 46: 9231–9240.

Waugh D, Garfinkel C, and Polvani L (2015) Drivers of the recent tropical expansion in the southern hemisphere: Changing SSTs or ozone depletion? *Journal of Climate* 28: 6581–6586.

Waugh D, Grise K, Seviour W, Davis S, Davis N, Adam O, Son S, Simpson I, Staten P, Maycock A, Ummenhofer C, Birner T, and Ming A (2018) Revisiting the relationship among metrics of tropical expansion. *Journal of Climate* 31: 7565–7581.

Woollings T, Franzke C, Hodson D, Dong B, Barnes E, Raible C, and Pinto J (2015) Contrasting interannual and multidecadal NAO variability. Climate Dynamics 45: 539–556.

Woollings T, Drouard M, O'Reilly C, Sexton D, and McSweeney C (2023) Trends in the atmospheric jet streams are emerging in observations and could be linked to tropical warming. Communications Earth & Environment 4: 125.

Wu Z and Reichler T (2020) Variations in the frequency of stratospheric sudden warmings in CMIP5 and CMIP6 and possible causes. Journal of Climate 33: 10305–10320.

Zaplotnik Ž, Pikovnik M, and Boljka L (2022) Recent Hadley circulation strengthening: A trend or multidecadal variability? Journal of Climate 35: 4157-4176.

Zhang W and Jin F-F (2012) Improvements in the CMIP5 simulations of ENSO-SSTA meridional width. Geophysical Research Letters 39: L23704.